Regular paper

Characterization of the indoor radio propagation channel at 2.4 GHz

Tadeusz A. Wysocki and Hans-Jürgen Zepernick

Abstract — The unlicensed industrial, scientific, and medical (ISM) band at 2.4 GHz has gained increased attention recently due to the high data rate communication systems developed to operate in this band. The paper presents measurement results of fading characteristics, multipath parameters and background interference for these frequencies. Some statistical analysis of the measured data is presented. The paper provides information that may be useful in design and deployment of communication systems operating in the 2.4 GHz ISM band, like those compliant with IEEE 802.11 standard and Bluetooth open wireless standard.

Keywords — indoor radiocommunication, microwave propagation, fading channels, jamming.

1. Introduction

Recently a number of data communication systems has been developed to utilize the unlicensed industrial, scientific, and medical band at 2.4 GHz [1]. The two most prominent examples of such systems are IEEE 802.11 wireless LAN [2], and personal area network employing Bluetooth enabled devices [3]. To assist in deploying of those systems, characterization of the indoor radio propagation channel at 2.4 GHz is essential. Measurement results for the indoor radio propagation channel have been presented in various publications. However, they tend rather to focus on a single characteristic, e.g. pulse propagation characteristic, as in [4], or temporal fading caused by motion of people and other objects within the channel [5], or simply deal with different frequency bands, like in [6].

In this paper, we present measurement results for the three major channel characteristics in the 2.4 GHz ISM band, i.e. temporal fading, channel impulse response, and background noise. The paper is organized as follows. Section 2 deals with the temporal fading characteristics. Example measurement results together with the cumulative distribution functions for typical measurements fitted to those of Rician distributions [7] are presented there. Level crossing rates and average duration of fades extracted from the measurements are included, too. Section 3 is devoted to the measurements of multipath channel parameters for the 2.4 GHz ISM indoor channel. In Section 4, the results of background interference measurements are shown, with microwave ovens indicated as major sources of an electromagnetic pollution in this band. Section 5 concludes the paper.

2. Fading characteristics

The measurements reported here were conducted at a laboratory of the Cooperative Research Centre for Broadband Telecommunications and Networking, Curtin University of Technology, Perth, Western Australia. The room topology is shown in Fig. 1. This environment was of relatively small dimensions being rectangular in size 7.8 m by 9.95 m within a three-metre ceiling. The ceiling was located 1.5 m below the steel reinforced concrete floor for the second storey of the four-storey building. The laboratory had two doorways and no windows. It had steel-framed walls clad with plaster-glass, a dropped ceiling constructed with non-metallic acoustic tiles, and a carpeted concrete floor. The laboratory was heavy cluttered with test and measurement equipment located on the benches.

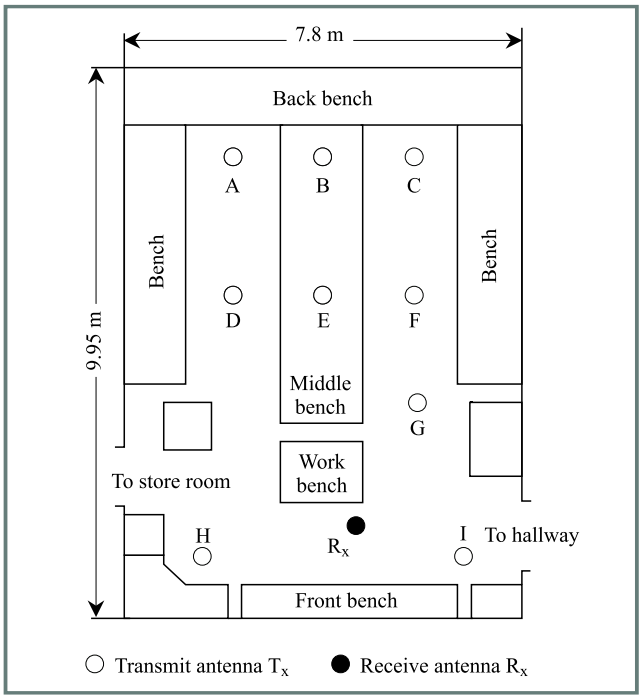

Fig. 1. Antenna placements for fading measurements.

2.1. Measurement procedure

We used the Hewlett Packard HP89441A to feed a quarter wave monopole antenna designed for the frequency range $2.3 \div 2.5$ GHz. The transmitter and the identical receiv-

ing antennas were mounted on two separate identical PVC pipes of heights adjustable in the range 1.0 to 2.0 m. At the receiver, a Marconi TF2300A modulation analyzer was applied to perform an envelope detection of the down converted baseband signal. The resultant signal was sampled, and the results stored on a hard disk for post-processing.

For all fading measurements, receive antenna R_x remained fixed and transmit antenna T_x was moved to different placements (Fig. 1). For each T_x placement and with no movement of people, the received signal was calibrated to -65 dBm. This receive level provided a signal to measurement system noise ratio of 35 dB, thus allowing fade depths of this order to be identified. To determine impairments caused by sources from outside the laboratory, we initially kept all motion in the room at zero. The variations of the received signal amplitude were less than ± 0.2 dB and could be regarded as insignificant. Then, we collected measurements for nine different transmit antenna locations with three people moving around the receive antenna only, keeping them within a two metre radius. The duration of measurements for each pair of antenna locations was twenty seconds. As an example, Fig. 2 shows a typical fading pattern observed with transmitt antenna T_x at the placement C.

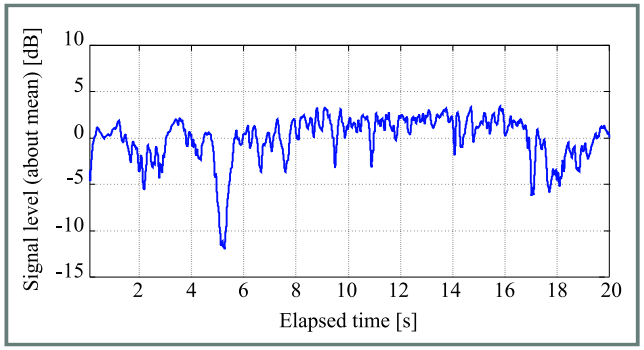

Fig. 2. Fading for transmit antenna at position C.

2.2. Fading distributions

In an indoor environment, we expect a line-of-sight path between transmit and receive antenna. Hence, the probability density function of the fast varying amplitude of the received instantaneous signal can be described by a Rician distribution. The probability that the received amplitude does not exceed a given threshold r is given by integration of the probability density function and is called cumulative distribution function $C(r)$. For curve fitting purposes, it is convenient to use the complementary cumulative distribution function $\overline{C}(r)$, which for a Rician distribution is given by [7]

$$\overline{C}(r) = 1 - C(r) =$$

$$= \exp\left[-\left(K + \frac{r^2}{2\sigma^2}\right)\right] \sum_{m=0}^{\infty} \left(\frac{\sigma\sqrt{2K}}{r}\right) I_m\left(\frac{r\sqrt{2K}}{\sigma}\right), \quad (1)$$

where $I_m(r)$ denotes the modified mth order Bessel function of the first kind, σ^2 is the local-mean scattered power, and K is called Rician factor specifying the ratio of power in the dominant path to power in the scattered path.

In calculating the empirical distribution functions, the measured data was classified into $\beta = 1.87(v-1)^{2/5}$ bins [8] where v is the number of samples collected in a measurement period. Then, a set of hypotheses for $\overline{C}(r)$ with $K = 0$ to $K = 15$ in 0.1 increments were tested to match the measured function. We applied the Kolmogorov-Smirnov goodness-of-fit technique for testing the relevance of match between measurement and hypothesis. Since the power level was normalized about median, a respective Rician factor K fully specifies a particular fading distribution. Table 1 shows the obtained Rician factors K.

Table 1
The Rician factors at various transmit antenna placements

Placement	A	B	C	D	E	F	G	H	I
K [dB]	2.79	8.19	9.86	5.95	8.80	3.80	8.26	7.85	5.79

Figure 3 shows curve fitting results for T_x at C. The large Rician factor of K = 9.86 dB indicates a strong line-of-sight path. Note also that the deviation between measured and matched distribution appears large for small power levels but is actually small due to scaling.

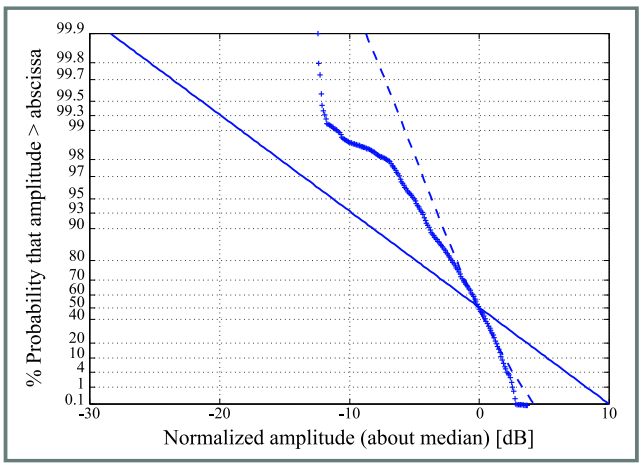

Fig. 3. Complementary cumulative distribution function $\overline{C}(r)$ for transmit antenna T_x at placement C; „+" fading measurement, „- -" Rician fading with K = 9.86 dB, „—" Rayleigh fading as reference.

2.3. Fading statistics

To design data and signaling formats for a wireless system, we require statistics which quantify the number of times a given threshold is crossed and the duration of time for which the signal is below that threshold. By counting all N crossings with positive slope at a given level L for mea-

surement period T, the level crossing rate can be computed as [9]

$$N_L = \frac{N}{T} . \tag{2}$$

The average duration of fades $\bar{t}_L$ in respect to level L and measurement period T is given by [9]

$$\bar{t}_L = \sum_{i=1}^{N} \frac{t_i}{N} , \tag{3}$$

where t_i is an ith fade duration, i.e. time for which the received signal is below a given level L. Table 2 displays fading statistics of selected fading measurements. Obviously, the average duration of very deep fades is rather short.

Table 2
Fading statistics for transmit antenna at selected placements

L [dB]	N_L [s^{-1}]			$\bar{t}_L$ [s]		
	C	E	I	C	E	I
6			0.101			9.868
3	0.554	2.195	2.526	1.765	0.363	0.290
0	1.308	2.147	3.183	0.295	0.141	0.118
-3	0.755	0.927	1.768	0.150	0.161	0.080
-6	0.151	0.781	0.859	0.158	0.121	0.092
-9	0.050	0.488	0.354	0.275	0.129	0.143
-12	0.050	0.439	0.303	0.008	0.092	0.131
-15		0.293	0.202		0.085	0.147
-18		0.195	0.202		0.091	0.110
-21		0.195	0.152		0.062	0.115
-24		0.098	0.152		0.069	0.079
-27		0.049	0.051		0.032	0.079

3. Multipath channel parameters

Delay profile measurements were conducted in the same laboratory as the fading measurements. However, this time the location of transmit antenna T_x remained fixed for all measurements, and the receive antenna R_x was placed at different locations within the laboratory. A plan view of the laboratory with the four antenna positions used for delay profile measurements is depicted in Fig. 4.

3.1. Delay profile measurements

Because of the confined environment, we could use the standard channel impulse response measurement system [10] based on the vector network analyzer HP 8753C equipped with an S-parameter test set HP 85046A. We used the same antennas as for the fading measurements. The results were recorded using HP VEE user interface and stored on a hard drive for post-processing. Albeit the 2.4 GHz ISM band spans from 2.4 to 2.485 GHz, we performed measurements in the band 2.1 to 2.8 GHz which gave us

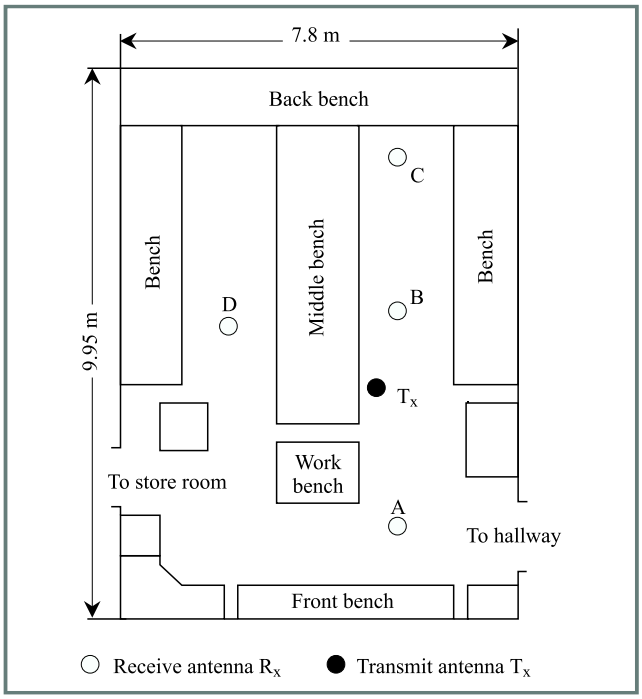

Fig. 4. Antenna placements for delay profile measurements.

a resolution of 837.05 mm, when normal window [11] was used. This translates into time resolution of 2.7921 ns.

During the measurement periods, three people kept moving in a similar manner around the receive antenna R_x, staying all the time within a two metre radius. Receive positions A, B and C were located within the left-hand aisle of the laboratory but with different distances to transmit antenna T_x. The specific characteristic of the receive position A was its direct vicinity to the nearby hallway which could cause additional scattering. In other words, time dispersion parameters at location A were expected to be of higher value than those observed at the three other locations. The particular feature of the receive location D was that the direct line-of-sight to the transmit antenna T_x did not exist because of the middle bench obstruction.

Figures 5 to 8 show the measured power delay profiles for the receive antenna R_x located at positions A, B, C, and D. The largest amplitude of each profile has been normalized to 0 dB.

3.2. Time dispersion parameters

It can be seen from the plots presented in Figs. 5 to 8 that a received wide-band signal will suffer spreading in time compared to the transmitted signal. This effect is called delay spread. Several delay-related parameters used for channel classification can be extracted from the measured power delay profile $P(\tau_\nu)$ where τ_ν denotes νth time instant.

The most commonly used time dispersion parameters are [12]:

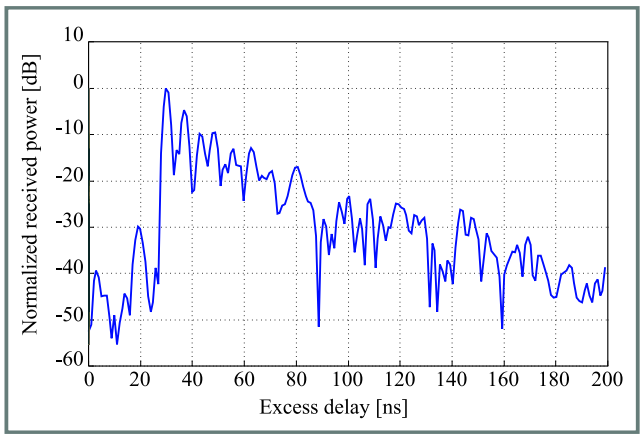

Fig. 5. Power delay profile for receive position *A*.

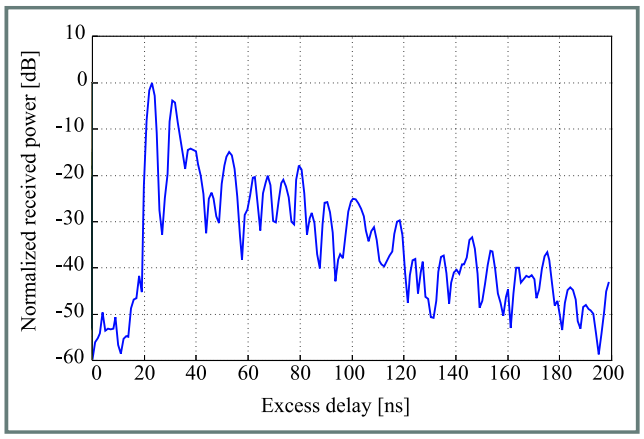

Fig. 6. Power delay profile for receive position *B*.

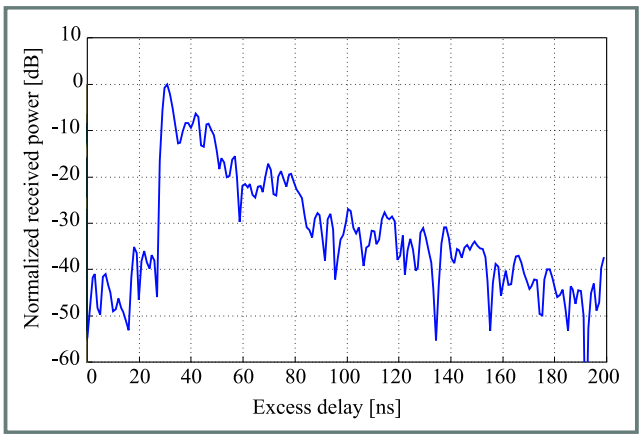

Fig. 7. Power delay profile for receive position *C*.

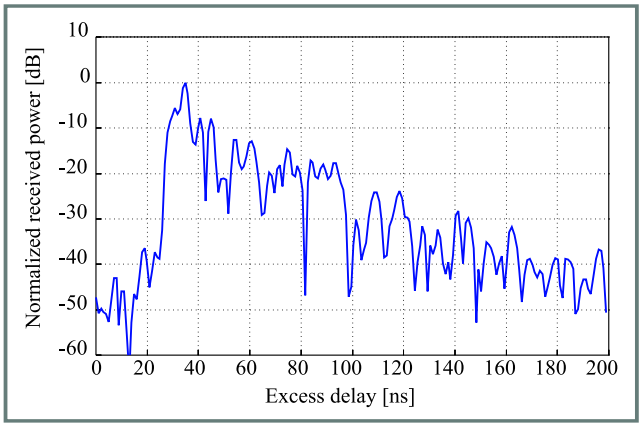

Fig. 8. Power delay profile for receive position *D*.

- Mean excess delay, which is the first moment of the power delay profile defined by:

$$m_\tau = \frac{\sum_\nu P(\tau_\nu)\tau_\nu}{\sum_\nu P(\tau_\nu)} \,. \tag{4}$$

- Root mean square (rms) delay spread, which is the square root of the second central moment of the power delay profile and is given by:

$$\sigma_\tau = \sqrt{\frac{\sum_\nu [\tau_\nu - m_\tau]^2 P(\tau_\nu)}{\sum_\nu P(\tau_\nu)}} \,. \tag{5}$$

- Maximum excess delay X [dB], defined as the time period during which the power delay profile falls to X [dB] below its maximum [10].

Note that mean excess delay and rms delay spread have to be computed with respect to a reasonable threshold for the multipath noise floor. If this threshold were set too low, it would result in too high values for these dispersion parameters. Our statistical analysis is based on a noise threshold set to four times of the noise standard deviation, which is known as a rule of thumb (as used in [13]). Numerically, the noise threshold was set to -34 dB with respect to the normalized receiver power.

A dual representation of delay spread in terms of a frequency domain parameter is given by the coherence bandwidth B_c. This parameter specifies the frequency range over which a transmission channel affects the signal spectrum nearly in the same way, giving an approximately constant attenuation and a linear change in phase. The coherence bandwidth is inversely proportional to rms delay spread. Assuming frequency correlation between amplitudes of frequency components being above 0.9, the coherence bandwidth can be approximated by [9]

$$B_c \approx \frac{1}{50\sigma_\tau} \,. \tag{6}$$

The time dispersion parameters extracted from the measured power delay profiles are summarized in Table 3. As we expected, the mean excess delay at receive position *A* is higher than at *B* and *C* which was assumed to be caused by multipath scattering into the nearby hallway. It is interesting to note that at the receive position *D*, we obtained the highest value of maximum excess delay in respect to 20 dB threshold from 0 dB power level. This is likely a result of the missing line-of-sight path at receive position *D*.

Table 3
Time dispersion parameters for receive antenna at various placements

Placement	A	B	C	D
Mean excess delay [ns]	57.04	43.40	49.10	54.85
Rms delay spread [ns]	30.55	24.12	22.19	26.82
Max excess delay 20dB [ns]	53.73	59.73	50.74	66.67
Coherence bandwidth [kHz]	654.66	829.19	901.31	745.71

4. Background interference

One of the important aspects of channel characterization is classification of noise and interference sources that need to be taken to account in the given bandwidth. This is particularly important in the case of unlicensed bands, as is the case of the 2.4 GHz ISM band, where users of wireless technologies operating in these bands are not required to obtain operating licenses provided that higher gain antennas are not used. On the other hand, there are no guarantees that the band is free of interference.

To identify the possible noise and interference sources that can affect use of the 2.4 GHz ISM band for communication purposes, we performed a series of measurements in some typical operating environments, including a university campus, a large shopping centre, and an industrial workshop. We used Hewlett Packard Spectrum Analyzer HP 8595E with a colinear antenna for omnidirectional measurements and a corner reflector antenna for directional measurements, i.e. when the particular source had been identified.

After conducting those measurements, we identified one major class of interference sources radiating in the 2.4 GHz ISM band, which were microwave ovens. Apart from that, the band was almost clear. The only other interference sources were building alarms as those used typically in businesses. Although only discovered in two cases from various measurement sites, they were found to output discrete frequency signals of moderate to low levels. The radiation came from the alarm units themselves (the most likely from oscillator circuits), and not the sensors, as they operated at infrared frequencies. A typical spectrum analyzer trace taken at a distance of 1 m from the alarm unit, with the directional corner reflector antenna is given in Fig. 9. The reading was obtained at Wilson's Engraving Works in Perth, Western Australia.

Microwave ovens were identified as major sources of interference at both the university environment and the shopping mall. The spectrum analyzer trace obtained from the 2 m measurements, using the directional corner reflector antenna and „peak-and-hold" function of the analyzer, is shown in Fig. 10. The plot presents raw data only. To derive the exact values of interference level from the trace it is necessary to account for system gains and losses.

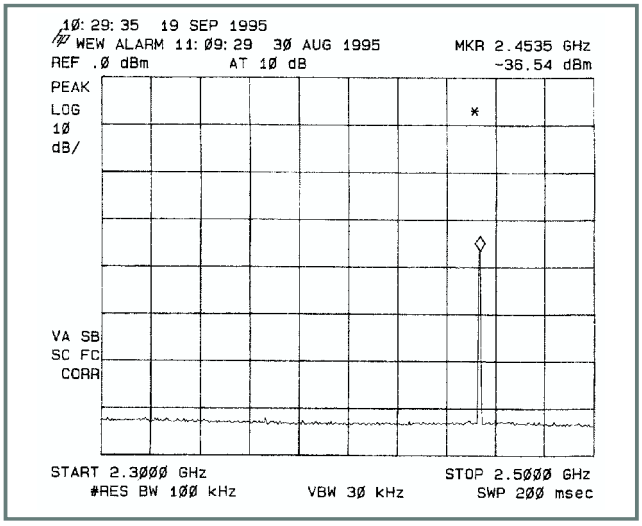

Fig. 9. Sample spectrum analyzer output for an alarm unit.

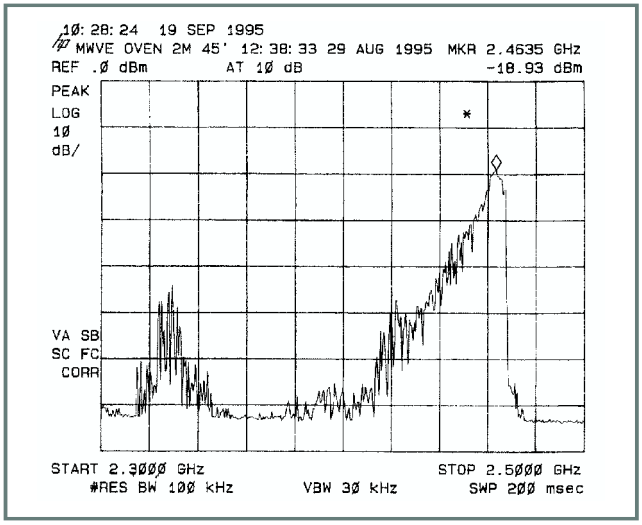

Fig. 10. Sample spectrum analyzer output for a single microwave oven at 2 m using the corner reflector antenna.

The plot of Fig. 10 shows a typical signature of the leakage output spectrum for a microwave oven. Brief analysis of two other microwave ovens, demonstrated that they at least (and presumably most others) share a similar signature of leakage output spectrum, both in intensity (related to efficiency and sealing of microwave) and spectrum occupation. Considering microwave ovens operating in multiplicity, the omnidirectional measurements were taken. This was deemed so, because of the multitude of signals and many reflective surfaces from which they could bounce in the Whitford City Shopping Centre Food Hall. It was impossible to selectively determine the source of any one signal since there were many food outlets operating microwave ovens simultaneously. Rather, the various microwave oven output signals combined producing a composite interference environment, that could only be measured with relevance with an omnidirectional antenna.

Figure 11 shows a typical output trace for the food hall environment. Once again, the trace provides us with a spectral

signature of the environment. It has the usefulness of providing a good indication of what spectrum one can expect in such a topology, with respect to frequency variation and interference intensity. The trace is actually similar to the one presented in Fig. 10, except that the noise is spread more evenly over the entire ISM band, as a result of the differing characteristics of the various microwave ovens. However, it is still possible to notice the peak in noise power between $2.4 \div 2.47$ GHz, which is directly coincident with the band of interest for microwave wireless LAN's.

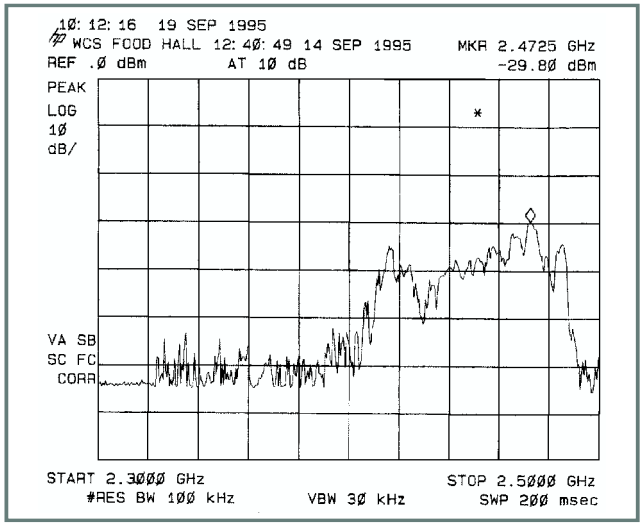

Fig. 11. Sample spectrum analyzer output for multiple microwave oven environment using omnidirectional antenna.

Both plots presented in Figs. 10 and 11 indicate that microwave ovens generate interference of a considerable level in the whole 2.4 GHz ISM band. The plots were obtained using „peak-and-hold" function of the analyzer. The instantaneous output of the analyzer revealed that the single operating microwave oven generated a single tone signal with the frequency hopping within the whole bandwidth. Therefore, one can expect the direct sequence (DS) spread spectrum (SS) devices, like DS mode of IEEE 802.11 wireless LAN, should perform quite well even in the close proximity to operating microwave ovens. On the other hand, the frequency hopping (FH) SS devices, like the Bluetooth compliant ones might experience difficulties in such an environment.

5. Conclusions

In this paper, we presented the measurement results, which can be used to characterize the 2.4 GHz unlicensed ISM band from the viewpoint of its usefulness for high data rate communications. The reported measurements deal with characteristics of fades and multipath channel parameters. In addition, special considerations are given to identifying possible sources of interference present in this band. The fading characteristics as well as multipath parameters were measured at one location that was a heavy cluttered laboratory. Thus, the presented results can be used to characterize indoor environment. The background interference measurements were performed at several different locations. The only major source of interference identified were microwave ovens, which based on the results, can have significant impact even on some SS systems. Because of the nature of this interference, it can be expected to particularly impair signal quality in FH SS systems, like Bluetooth enabled devices.

References

[1] V. K. Garg, K. Smolik, and J. E. Wilkes, *Applications of CDMA in Wireless/Personal Communications*. Upper Saddle River: Prentice Hall, 1997.

[2] „IEEE 802.11 Standard for Wireless LAN", IEEE Standards Department, New York, 1997.

[3] J. Haartsen *et al.*, Bluetooth Specification Version 1.0, Part B, Baseband Specification, 1999.

[4] S.-C. Kim, H. L. Bertoni, and M. Stern, „Pulse propagation characteristics at 2.4 GHz inside buildings", *IEEE Trans. Veh. Technol.*, vol. VT-45, no. 3, pp. 579–592, 1996.

[5] E. Walker, H.-J. Zepernick, and T. Wysocki, „Fading measurements at 2.4 GHz for the indoor radio propagation channel", in *1998 Int. Zurich Sem. Broadband Commun.*, Zurich, Switzerland, Feb. 1998, pp.171–176.

[6] H. Hashemi, M. McGuire, T. Vlasschaert, and D. Tholl, „Measurements and modelling of temporal variations of the indoor radio propagation channel", *IEEE Trans. Veh. Technol.*, vol. VT-43, no. 3, pp. 733–737, 1994.

[7] R. Steele, *Mobile Radio Communications*. New York: IEEE Press, 1994.

[8] J. S. Bendat and A. G. Piersol, *Measurement and Analysis of Random Data*. New York: Wiley, 1966.

[9] W. C. Y. Lee, *Mobile Communication Design Fundamentals*. New York: Wiley, 1993.

[10] T. S. Rappaport, *Wireless Communications – Principles and Practice*. New York: IEEE Press, 1996.

[11] „HP 9753C Network Analyzer Operating Manual", Hewlett-Packard, USA, 1990.

[12] T. Wysocki, H.-J. Zepernick, and R. Weber, „Mobile Communications", in *Wiley Encyclopedia of Electrical and Electronics Engineering*, J. G. Webster, Ed. New York: Wiley, 1999, vol. 13, pp. 343–353.

[13] D. Lacroix, C. L. Despins, G. Y. Delisle, P. Marinier, and P. Luneau, „Experimental characterization of outdoor microcellular quasi-static channels in the UHF and SHF bands", in *Proc. IEEE ICCC'97*, Montreal, CD, June 1997.

Tadeusz A. Wysocki received the M.Sc.Eng. degree with the highest distinction in telecommunications from the Academy of Technology and Agriculture, Bydgoszcz, Poland, in 1981. In 1984, he received his Ph.D. degree, and in 1990, was awarded a D.Sc. degree (habilitation) in telecommunications from the Warsaw University of Technology. In 1992, Dr. Wysocki moved to Perth, Western Australia to work at Edith Cowan University. He spent the whole 1993 at the University of Hagen, Germany, within the framework of Alexander von Humboldt Research Fellowship. After returning to Australia,

he was appointed a Project Leader, Wireless LANs, within Cooperative Research Centre for Broadband Telecommunications and Networking. Since December 1998 he has been working as an Associate Professor at the University of Wollongong, NSW, within the School of Electrical, Computer and Telecommunications Engineering, being a Research Coordinator of the Switched Networks Research Centre. The main areas of Dr. Wysocki's research interest include: indoor propagation of microwaves, code division multiple access (CDMA), digital modulation and coding schemes as well as mobile data protocols including those for ad-hoc networks. He is the author or co-author of three books, over 100 research publications and nine patents. He is a Senior Member of IEEE.
e-mail: Wysocki@uow.edu.au
School of Electrical
Computer and Telecommunications Engineering
University of Wollongong
NSW 2251

Hans-Jürgen Zepernick received the Dipl.-Ing. degree in electrical engineering from the University of Siegen, Germany, in 1987. He then was with the Radio and Radar Department of Siemens AG, Munich, Germany. From August 1989 until April 1995, he was with the Department of Communications Engineering at the University of Hagen, Germany, researching into the areas of mobile communications and error control coding. In 1994, he received the Dr.-Ing. degree. In 1995, he joined the Cooperative Research Centre for Broadband Telecommunications and Networking in Perth, Australia, as a Research Fellow working in the Wireless ATM project on physical layer topics. He is an author or co-author of some 45 technical papers. His research interests include radio channel characterisation and modelling, coding and modulation, equalisation, spread-spectrum systems, wireless networks and third generation wireless systems.
e-mail: Hans@atri.curtin.edu.au
Australian Telecommunications Research Institute
Curtin University of Technology